

equations for the pendulum if corresponding simplifying assumptions are made. In the pulsed pendulum tests, the increase in the maximum velocity at bottom dead center was used to deduce the thrust. The criticality of pulse position was examined analytically using Eqs. (5) and (6). This was done by permitting a free swing to a given position, starting a new solution at that point for pulsed operation with the free swing terminal boundary conditions  $(\theta_0, \dot{\theta}_0)$ , and then renewing the solution for free swing again with terminal boundary conditions from the pulsed period. The curve developed from this information (Fig. 2) indicated that for the conditions examined the measured velocity increase would be relatively insensitive to pulse position with  $\pm 5^\circ$  of bottom dead center. During the tests all pulses were initiated  $\pm \frac{1}{4}^\circ$  of bottom dead center. In reducing the data from this latter case, note that Eq. (6) with the initial condition  $\theta_0 = 0$  becomes

$$\dot{\theta} = \dot{\theta}_0 \cos At - (B/A) \sin At \quad (7)$$

and, for small values of  $At$ , this becomes

$$\dot{\theta} - \dot{\theta}_0 = -Bt_p \quad (8)$$

where  $t_p$  = duration of pulse (valve open time). Thus, the measured velocity change  $(\Delta v)$  at bottom dead center before and after a pulse is

$$\Delta v = Bt_p t_p = (F_e t_p) l/l_p g/Wk_0^2 \quad (9)$$

or

$$I_b = (F_e t_p) = Wk_0^2 \Delta v / l/l_p g \quad (9a)$$

where  $I_b$  is the integrated impulse bit applied during a pulse and  $F_e$  is the "effective thrust" defined as

$$F_e \equiv I_b/t_p \quad (10)$$

Checks of the simplifying assumptions in Eq. (9a) indicate that errors greater than 1% are not introduced. In the tests  $v_{\max}$  at bottom dead center was not measured but rather the average velocity over the distance between the photocells. This small correction can be defined precisely as a function of observed time increments. Appropriate corrections were applied to all data.

The radius of gyration was deduced from the natural period of the pendulum, and the center of gravity was determined experimentally. A slight shift in these quantities took place as gas was used from the bottle, but this was a small correction that was easy to apply. In Table 1, the characteristics of the pendulum actually used are given.

### Pulsed Rocket Tests

Runs were made with the pendulum installed in an extreme altitude chamber. Swings were initiated by pulsing the valve, and data were recorded under a variety of pulse durations until the storage bottle charge was exhausted.

Specific impulse was determined by dividing the total impulse per pulse ( $I_b$ ) by the flow of propellant per pulse. This latter value was obtained by an independent weighing calibration for a large number of pulses. Typical data from the program are given in Table 2.

### Summary

The performance of small pulsed rocket motors can be measured effectively by using a swinging pendulum. The measurement fundamentally is grounded in well-defined pendulum behavior. Such a pendulum can be built inexpensively, with masses and lengths adjusted to produce the desired accuracy.

### Reference

- 1 Azeltine, J. A., *Transform Methods in Linear System Analysis* (McGraw-Hill Book Co. Inc., New York, 1958), p. 22.

## Radial Viscous Free-Mixing

MARTIN H. STEIGER\*

*Polytechnic Institute of Brooklyn, Farmingdale, N. Y.*

### Introduction

VISCOUS laminar and turbulent compressible radial jets (i.e., motionless ambient) and wakes are investigated by a boundary-layer type of analysis with integral methods. A schematic diagram of radial free-mixing is presented in Fig. 1. The radial jet, for example, can be produced by two circular jets of equal strength, which are directed at one another and, after impact, spread out radially. Other types of radial free-mixing can be produced by flows issuing (or being absorbed) through perforations around the circumference of a right circular cylinder. Studies of radial flow have been restricted to laminar jets<sup>1, 2</sup> and laminar jets with an axisymmetric weak swirl.<sup>2</sup>

### Analysis

The following boundary-layer equations are assumed to govern the viscous free-mixing previously discussed and represented schematically in Fig. 1:

Continuity

$$(\rho u x)_x + (\rho v x)_r = 0 \quad (1)$$

Momentum

$$\rho u u_x + \rho v u_r = (\mu u)_r \quad (2a)$$

$$p = \text{const} \quad (2b)$$

where  $x$  and  $r$  are the radial and normal coordinates with velocity components  $u$  and  $v$ ,  $p$  denotes pressure,  $\rho$  density,  $\mu$  coefficient of viscosity, and subscripts  $x$  and  $r$  denote partial differentiation with respect to the indicated variable.

Equations (1) and (2) govern either laminar flow or the mean quantities of turbulent flow if, in the turbulent case, the transport variable  $\mu$  is interpreted to be the eddy coefficient of viscosity. Turbulent considerations are handicapped by a dearth of knowledge concerning the behavior of the eddy viscosity in compressible flows. Here it is suggested that the eddy viscosity may be assumed in the form

$$\epsilon_v = K \delta_m \rho_0 |u_e - u_0| \quad (3)$$

where  $K$  is a constant,  $\delta_m$  is the transformed viscous layer thickness [Eq. (6)], and subscripts  $e$  and  $0$  denote conditions at the edge of the viscous-layer and quantities evaluated at the symmetric axis (i.e., at  $r = 0$ ), respectively. In order to be able to treat both wakes and jets, the absolute value of  $|u_e - u_0|$  should be taken. Equation (3) gives the proper behavior in the incompressible limit.

The boundary conditions are

$$\text{at } r = 0 \quad u_r = v = 0 \quad (4a)$$

$$\text{at } r = \delta \quad u = u_e = \text{const} \quad (4b)$$

Solutions are derived by applying the simple one-strip integral method, which consists of satisfying the momentum integral equation [derived by integrating (2) with respect to  $r$  and using Eqs. (1) and (4)], namely,

$$\int_0^\delta \rho u |u_e - u| x dr = \theta_c = \text{const} \quad (5a)$$

and the momentum equation evaluated along the  $x$  axis

$$\rho_0 u_0 (du_0/dx) = \mu_0 u_{rr0} \quad (5b)$$

Received March 27, 1963. The study was supported partially by the Air Force Office of Scientific Research Grant No. AF-AFOSR-1-63.

\* Research Associate, Graduate Center. Member AIAA.

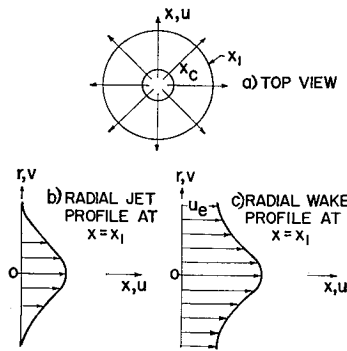


Fig. 1 Schematic diagram

where subscript  $c$  denotes conditions at an initial station.

The following boundary-layer compressibility transformation and velocity profile are used:

$$\bar{\rho} dr = \delta_m dn \quad (6a)$$

$$r = \delta_m \int_0^n \frac{dn}{\bar{\rho}} \quad (6b)$$

$$\delta = \delta_m \int_0^1 \frac{dn}{\bar{\rho}} \quad (6c)$$

and

$$u = u_0 + (u_e - u_0)f(n^2) \quad (7)$$

where  $\bar{\rho}$  denotes the density divided by its reference value (to be defined),  $f(n^2)$  is some function of  $n^2$ , and  $u_0 = u_0(x)$ .

The solutions are presented below.

#### A. Radial jets $u_e = 0$

##### A1. Laminar flow

$$\frac{3f''(0)}{(\rho_0 u_0 \delta_m^2 x^2 / \mu_0)_c} = \left[ 1 - \left( \frac{u_{0c}}{u_0} \right)^3 \right] \quad (8)$$

where  $\bar{\rho} = \rho / \rho_{0c}$ ,  $\bar{\mu} = \mu / \mu_{0c}$ , and  $f''(0) = (d^2 f / dn^2)_0$ .

##### A2. Turbulent flow

$$\frac{2Kf''(0)}{x_c \delta_{mc}} \int_{x_c}^x \bar{\rho}_0^2 x dx = \left[ 1 - \left( \frac{u_{0c}}{u_0} \right)^2 \right] \quad (9)$$

#### B. Radial wakes ( $u_e = \text{const not equal to zero}$ )

##### B1. Laminar flow

$$\frac{f''(0)}{\rho_e u_e \theta_c^2 / \mu_e} \int_{x_c}^x \bar{\rho}_0 \tilde{u}_0 x^2 dx = F(\tilde{u}_0) - F(\tilde{u}_{0c}) \quad (10a)$$

where  $\bar{\rho} = \rho / \rho_e$ ,  $\tilde{\mu} = \mu / \mu_e$ ,  $\tilde{u} = u / u_e$ , and

$$F(\tilde{u}_0) =$$

$$\frac{2B(2A - B)\tilde{u}_0^2 + (2A - B)(A - 3B)\tilde{u}_0 + A(5B - A)}{2(A + B)^3(1 - \tilde{u}_0)^2(A + B\tilde{u}_0)} + \frac{B(B - 2A)}{(A + B)^4} \ln \left( \frac{A + B\tilde{u}_0}{1 - \tilde{u}_0} \right) \quad (10b)$$

The constants  $A$  and  $B$  only depend on the functional form of  $f(n^2)$  and are defined as

$$A = \int_0^1 f(1 - f) dn \quad B = \int_0^1 (1 - f)^2 dn \quad (10c)$$

##### B2. Turbulent flow

$$\frac{Kf''(0)}{\theta_c} \int_{x_c}^x \bar{\rho}_0^2 x dx = G(\tilde{u}_0) - G(\tilde{u}_{0c}) \quad (11a)$$

Table 1 Asymptotic behavior of flow variables

	Laminar flow		Turbulent flow	
	$a$	$b$	$a$	$b$
Radial jet	-1	+1	-1	+1
Radial wake	$-\frac{3}{2}$	$+\frac{1}{2}$	-1	0

where

$$G(\tilde{u}_0) = \frac{-3B^2\tilde{u}_0^2 + 2(A^2 + AB + 3B^2)\tilde{u}_0 - (A^2 + 2B^2)}{2(A + B)^3(1 - \tilde{u}_0)^2} + \frac{A^2 + B^2 + AB}{(A + B)^3} \ln \left( \frac{A + B\tilde{u}_0}{1 - \tilde{u}_0} \right) \quad (11b)$$

It is of interest to examine the downstream asymptotic (i.e., as  $x \rightarrow \infty$ ) behavior of the velocity along the symmetric axis ( $u_0$ ) and the semiviscous-layer thickness ( $\delta$ ). If the effect of compressibility can be neglected, the forementioned solutions yield  $u_0 \sim x^a$ ,  $\delta \sim x^b$  for the jet and  $(u_e - u_0) \sim x^a$ ,  $\delta \sim x^b$  for the wake. Table 1 presents the values of the exponents associated with each of the various types of flows considered herein.

#### References

- <sup>1</sup> Squire, H. B., "Radial jets," *50 Jahre Grenzschichtforschung*, edited by H. Görtler and W. Tollmien (Braunschweig, Vieweg, 1955), pp. 47-54.
- <sup>2</sup> Riley, N., "Radial jets with swirl," *Quart. J. Mech. Appl. Math.* 15, 435-469 (1962).

## Vortices in Solid Propellant Rocket Motors

J. SWITENBANK\* AND G. SOTTER†  
University of Sheffield, Sheffield, England

#### Introduction

STUDIES of combustion instability in solid propellant rocket motors currently underway at the High Intensity Combustion Laboratory at Sheffield University have revealed an interesting interaction between the flow pattern and the combustion chemistry. This takes the form of strong vortices in the acoustic cavity which lead to several remarkable effects.

The possible occurrence of these vortices was proposed, largely on theoretical grounds, in an earlier study,<sup>1</sup> and subsequent experimental work has confirmed their existence.

#### Experimental Evidence

High-speed cinéphotos (1000 to 3200 frames/sec) have been taken which show that at least some of the unstable burning pressure peaks are associated with vortices in the flow. Figure 1a shows a typical vortex that filled the entire chamber. From visual observation, the circumferential gas speed is estimated at Mach 0.2 at the fore end, where the picture was taken. The vortex can be expected to gain strength downstream.

Received April 2, 1963. The authors wish to express their thanks to Imperial Metal Industries Ltd., Kidderminster, and to the Ministry of Aviation, who have sponsored this work. The assistance of J. Badger also is acknowledged.

\* Lecturer, Department of Fuel Technology and Chemical Engineering.

† Postgraduate Student, Department of Fuel Technology and Chemical Engineering.